International Journal of Engineering Applied Sciences and Technology, 2018
Vol. 3, Issue 9, ISSN No. 2455-2143, Pages 37-42
Published Online January 2019 in IJEAST (http://www.ijeast.com)

HIGH TEMPERATURE TENSILE PROPERTIES, STRAIN-INDUCED MARTENSITIC TRANSFORMATION, PLASTIC ANISOTROPY AND FORMABILITY OF AISI 304 METASTABLE AUSTENITIC STAINLESS STEEL

A. Kanni Raj
School of Basic Sciences
Vel Tech Rangarajan Dr.Sagunthala R&D Institute of Science & Technology
Chennai, Tamil Nadu, India

Abstract— **Tensile properties, martensitic formation and formability of sheets of two AISI 304 stainless steel sheets were evaluated. Both the sheets showed a similar type of tensile behavior. Ductility of the 1.25mm thick sheet was greater than that of the 0.5mm thick sheet. Tensile property parameters decreased, displaying a drastic decrease above 673K mainly on account of a decrease in work hardening. It displayed very good ductility at 373K due to the absence of both martensite formation and dynamic strain aging. At any particular strain, amount of martensite formed was more in the 1.25mm thick sheet. Normal anisotropy of 0.5mm thick sheet was high and expected to show somewhat greater deep drawability. Formability of 0.5mm thick sheet was lower in the stretch forming and plane strain forming conditions, but was superior in deep drawing region, when compared to that of 1.25mm thick sheet. Formability of both the sheets decreased at high biaxial strains due to the saturation and slowing down of the martensite formation. The plot of the constraint factor was steep in the case of the 0.50mm thick sheet compared with the 1.25mm thick sheet due to the larger strain gradients present in the former steel.**

Keywords—**Formability, Martensitic Transformation, Plastic Anisotropy, Tensile Properties**

I. INTRODUCTION

AISI 304 stainless steel is used extensively, especially in the manufacture of household utensils, in turn extensively studied material, even today research is done on its formability [Hecker et al.(1982), Murr et al.(1982), Narutani (1989), Date et al.(1992), Cios et al.(2017), Dutoit et al. (2012), Satao et al.(2014), Jayahari et al.(2014), Sivam et al (2015), Dehghani et al.(2016), Reddy (2017), Andrade et al.(2014), Sahu et al.(2018)], and is used to benchmark formability of AISI 200 series stainless steels. This steel is metastable and undergoes strain-induced martensitic transformation during uniaxial tensile testing at various strain rates. Hecker et al have studied this transformation as a function of temperature, strain rate and strain (stress) state. Modeling of the kinetics of martensite formation has also been attempted [Hecker et al.(1982)] . Both shear and normal stresses cause martensitic transformation. Murr et al have studied systematically how the microstructure (particularly α'-martensite) is determined by strain, strain rate and strain state [Murr et al.(1982)]. The strengthening effect of strain-induced martensite is well-known but its influence on formability is less understood. In some situations, martensite formation during straining has enhanced formability [Hecker et al.(1982), Murr et al.(1982)].

In many earlier research articles, the author authored many works on mechanical properties and formability of austenitic stainless steel sheets. In a recent study of the present author, on room temperature formability of two grades of AISI 304 austenitic stainless steel sheets was explained in detail. In this paper, high temperature tensile properties, strain-induced martensitic transformation, plastic anisotropy and room temperature formability of two AISI 304 austenitic stainless steel sheets are examined briefly [Kanniraj(2008)]. Steel sheets were supplied by Salem Stainless Steel Plant (Steel Authority of India Limited, Ministry of Steel, Government of India) under the aegis of Indian Stainless Steel Development Association (ISSDA), New Delhi, India.

II. MATERIALS & METHOD

Tensile tests were conducted on a 400kN Schenck servohydraulic testing machine (made in Germany, available in Indian Institute of Technology Madras) at a constant crosshead speed of 0.5mm/min (initial strain rate=0.00028/s) on ASTM E8M subsize specimens. The standard tensile properties, namely, 0.2% yield strength (YS), ultimate tensile strength (UTS), uniform elongation (e_u), total elongation (e_t), strain hardening exponent (n) were determined from load-elongation date. Strain rate sensitivity index (m) was calculated from strain rate jump tests using ASTM A370

International Journal of Engineering Applied Sciences and Technology, 2018
Vol. 3, Issue 9, ISSN No. 2455-2143, Pages 37-42
Published Online January 2019 in IJEAST (http://www.ijeast.com)

specimens. The crosshead speed was changed from 0.1mm/min (initial strain rate=0.00014/s) to 1.1mm/min (initial strain rate=0.00015/s). High temperature tests are carried out on another universal testing machine with tubular furnace attached to heat specimen (250kN Schenck-Trebel electromechanical testing machine, made in Germany, available in Indian Institute of Technology Madras). The tests are planned at various temperatures (373K, 473K, 573K, 673K, 773K and 873K) only for 0.50mm thick sheets on ASTM A370 subsize specimen used to evaluate high temperature tensile properties for AISI 304 sheets of SAIL Salem origin. Plastic anisotropy parameters – normal anisotropy or average plastic strain ratio (r_m) and planar anisotropy (Δr) were determined on a 400kN Schenck servohydraulic testing machine at a constant crosshead speed of 1mm/min (initial strain rate=0.00083/s). Cupping values were evaluated on a Erichsen cup tester using a blank holder pressure of 10kN. The maximum draw forces were 19kN and 30kN respectively for the 0.50mm thick and the 1.25mm thick sheets [Kanniraj(2018)].

Forming limit diagram (FLD) was evaluated following Hecker's simplified punch-stretching technique [Kanniraj(2018)]. Details on grid marking, punch-stretching and strain measurements are given elsewhere. (Experiments were done on Becker van Hullen 2000kN hydraulic double acting press, made in Germany, available in Indian Institute of Technology Madras.) The principal surface strains – major strain (e_1) and minor strain (e_2) – were measured using a transparent plastic scale from the selected safe (only undergone diffuse necking), necked (undergone localized necking) and failed (undergone splitting) ellipses in the blanks of eight different widths, subjected to biaxial stressing and ASTM E8M full size tensile specimens. The e_1-e_2 (strain space) diagram was plotted using the data points. A least squares polynomial regression analysis was carried out using the spread sheet software MS Office Excel only on the data points corresponding to the necked ellipses and the ellipses near the transition from safe to fractured regions. The degree of the polynomial is chosen in such a way that the error in the coefficients is minimal. The analysis is done separately for the left hand side (negative minor strain regime) and the right hand side (positive minor strain regime) of the FLD in order to minimise the standard error in the coefficients. Standard error is calculated by taking standard deviation as a criterion using the following equation. The experimental error limits are computed. Strain distribution profiles were also plotted. Constraint factor was used to analyse strain distributions in detail mathematically.

III. Results & Discussion

Table-1 presents the chemical composition of the two sheets. The 1.25mm thick sheet contained more Cr and Ni but less C compared to 0.50mm thick sheet. And also, it is expected to show increased ductility and formability. Grain sizes of the 0.5mm and 1.25mm thick sheets were 13±4μm and 14±3μm respectively. The difference in grain sizes was too small to have any effect on the properties. Table-2 compares the tensile properties of both the sheets. Differences between the YS and the UTS values of both the sheets were negligible. In both sheets, the UTS to YS ratios were approximately 2.73. The n values were similar too. Total elongation of the 0.5mm thick sheet was about 45% less than that of the 1.25mm thick sheet. An important reason for this difference was that the width of a neck is directly related to the sheet thickness. So, with increasing sheet thickness, more neck transforms into a localized neck. Both the sheets displayed a similar type of room temperature flow curves.

Table-1 Chemical composition (in Weight %) of the Two Sheets

Sheet Thickness (mm)	C	Cr	Ni	Mn	N	O	Co	Fe
0.5	0.06	17.8	8.47	1.57	0.015	0.129	0.139	Balance
1.25	0.04	18.5	9.24	1.56	0.017	0.125	0.178	Balanace

Table-2 Room Temperature Tensile Properties of the two Sheets (Initial Strain Rate=0.00028/s)

Sheet Thickness (mm)	Property in different directions	*YS (MPa)	UTS (MPa)	e_u	e_t	$^{\wedge}$n	K (MPa)	$^{+}$m
0.5	X_0	270	734	36	37	0.49	1738	0.012
	X_{45}	254	715	43	44	0.46	1592	0.012
	X_{90}	271	691	37	38	0.46	1580	0.012
	$^{\#}$Xm	262	714	40	41	0.47	1626	0.012
1.25	X_0	266	794	63	70	0.5	1604	0.011
	X_{45}	264	700	69	75	0.52	1557	0.012
	X_{90}	264	689	72	76	0.55	1628	0.012
	$^{\#}$Xm	264	721	68	74	0.52	1587	0.012

*0.2% offset
^n values are reported to 2 decimals, based on an error analysis (range of standard deviation 0.003-0.009)
$^{\#}Xm=(X_0+2X_{45}+X_{90})/4$ (where X is the property of interest). The suffixes denote the angle between tensile axis and sheet rolling direction.
$^{+}$m values are reported to 3 decimals, because the variations in this parameter were observed only in the third decimal. The strain rates before and after the jump were respectively 0.00014/s and 0.0015/s.

International Journal of Engineering Applied Sciences and Technology, 2018
Vol. 3, Issue 9, ISSN No. 2455-2143, Pages 37-42
Published Online January 2019 in IJEAST (http://www.ijeast.com)

The high temperature tensile properties are presented in Table-3. As the temperature is increased, the strength parameters (YS, UTS and K) and ductility parameters (e_u and e_t) show decrease, displaying a drastic decrease above 673K mainly on account of a decrease in work hardening. Even at elevated temperatures, AISI 304 show good work hardening capacity (data analysis is upto 873K), and it displays very good ductility at 373K. The very high value of the observed ductility at 373K is due to the absence of both martensite formation and dynamic strain aging (DSA) [Hecker et al.(1982), Murr et al.(1982)]. In brief, the changes in tensile properties with temperature are extremely complicated. In a qualitative sense, they may be understood in terms of changes in composition, the extent of martensite formation, magnitudes of the strain hardening index and the strain-rate sensitivity index, presence or absence of dynamic strain ageing and sheet thickness. Detailed systematic studies are necessary before the effects of each of these variables on the tensile properties can be quantified.

Table-3 High Temperature Tensile Properties of 0.5mm Thick Sheet (Initial Strain Rate=0.00069/s)

T(K)	YS (MPa)	UTS (MPa)	e_u	e_t	n	K (MPa)	m
298	275	734	36	37	0.49	1738	0.012
373	189	553	53	61	0.59	1429	0.03
473	175	480	36	41	0.44	1111	0.029
573	159	461	33	34	0.5	1171	0.025
673	143	457	33	35	0.51	1166	0.028
773	139	424	28	30	0.5	1115	0.027
873	122	332	33	33	0.49	841	0.036
Specimen with tensile axis along sheet rolling direction was used, as slight or no variation of tensile properties due to texture and grain orientation are possible at high temperature.							

At any particular strain, the amount of martensite formed was more in the 1.25mm thick sheet than the 0.5mm thick sheet (Fig.1). The amount of strain-induced martensite formed (measured in terms of the ferrite number, FN) could be described by a polynomial in per cent uniaxial true tensile strain by the following relations (Equations 1 & 2 respectively for 0.5mm thick and 1.25mm thick sheets).

$$FN = 0.753 - 0.221\varepsilon + 0.0097\varepsilon^2 \quad (1)$$

$$FN = 2.62 - 1.112\varepsilon + 0.0601\varepsilon^2 - 0.0005\varepsilon^3 \quad (2)$$

The amount of martensite formed a a function of maximum principal biaxial true strain and von Mises effective strain are presented in Fig.2. (Data corresponding to uniaxial tensile testing are also shown for comparison.) The amount of strain-induced martensite formed as a function of von Mises effective strain, ε_{vM}, could be described by the following relations (Equations 3 & 4 respectively for 0.5mm thick and 1.25mm thick sheets).

$$FN = 0.443 - 0.097\varepsilon_{vM} + 0.0036\varepsilon_{vM}^2 - 0.000025\varepsilon_{vM}^3 \quad (3)$$

$$FN = 2.0012 - 0.436\varepsilon_{vM} + 0.0135\varepsilon_{vM}^2 \quad (4)$$

It is seen from Fig.2 that in biaxial tension martensite formation is twice as fast as under uniaxial tension. The plastic anisotropy parameters are given in Table-4. The r_m values of the 0.5mm thick sheet (subjected to greater cold work) was 10% greater than that of the 1.25mm thick sheet. Therefore, the 0.5mm thick sheet is expected to show somewhat greater deep drawability, and could be established in terms of forming limit diagrams also. Δr value of the 0.5mm thick sheet was nearly thrice as much as that of the 1.25mm thick sheet, and hence, the 0.5mm thick sheet is expected to show more earing than the 1.25mm thick sheet. (No experiments were conducted to determine the extent of earing in the two sheets.)

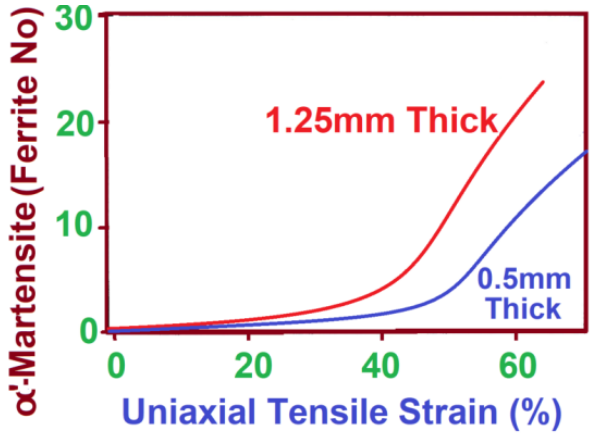

Fig.1 Amounts of α'-Martensite Formed as a Function of Uniaxial Tensile True Strain in the 0.5mm Thick and the 1.25mm Thick Sheets

International Journal of Engineering Applied Sciences and Technology, 2018
Vol. 3, Issue 9, ISSN No. 2455-2143, Pages 37-42
Published Online January 2019 in IJEAST (http://www.ijeast.com)

Erichsen cup depths were 12.3mm and 12.9mm respectively for 0.5mm and 1.25mm thick sheets. This is a parameter devoid of much scientific meaning. However, as it appears in all specifications on sheet steels these values have been reported here for completeness [Kanniraj(2008)].

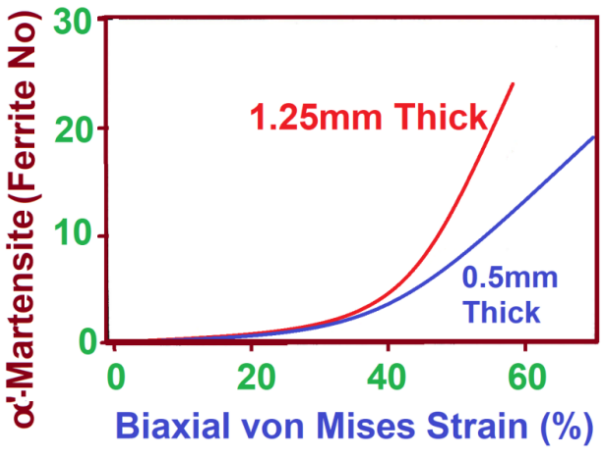

Fig.2 Amounts of α'-Martensite formed as a function of Biaxial von Mises Effective Strain in the 0.5mm thick and the 1.25mm thick sheets

Forming limit diagrams of the 0.5mm and the 1.25mm thick sheets were constructed by a quadratic least square analysis for the left hand side (deep drawing region) and cubic least square analysis for the right hand side (biaxial stretching region). The standard errors in the forming limit curves were 3.8% and 1.7% respectively in the case of the 0.5mm thick and 1.25mm thick sheets. The higher error in the thinner specimen was associated with the greater difficulty in the identification of necking in sheets of lower thickness. A comparison of the mean forming limit diagrams of the 0.5mm and the 1.25mm thick sheets is given in Fig.3. (Failure indicated by these curves represents the onset of localized necking. But during biaxial testing, in both the sheets necking could not be easily distinguished from fracture due to the extremely limited post-necking strain present.)

Table-4 Plastic Anisotropy Prtoperties of the Two Sheets (Initial Strain Rate=0.00028/s)

Sheet Thickness (mm)	r_0	r_{45}	r_{90}	$^{\#}r_m$	$^{*}\Delta r$
0.5	0.77	1.30	0.97	1.09	-0.43
1.25	0.83	1.03	0.96	0.96	-0.14
#normal anisotropy or average plastic strain ratio, $r_m=(r_0+2r_{45}+r_{90})/4$ *planar anisotropy, $\Delta r=(r_0-2r_{45}+r_{90})/2$. Suffixes denote angle between tensile axis and sheet rolling direction.					

In general, formability in all modes of deformation increases with increasing sheet thickness. But, in the present experiments the formability of the thicker sheet did not exceed that of the thinner sheet by more than 5%. But the forming limit curve for the 0.5mm thick sheet extended well beyond -10% minor strain revealing the greater deep drawability of this sheet. In contrast, the forming limit curve of the 1.25mm thick extended beyond a minor strain of +13% which indicated its greater biaxial stretchability. In and near the plane strain forming conditions the formability of both sheets was similar as their mean lines lay within experimental error limits of the 0.5mm thick sheet. Formability decreased at extreme biaxial strains because of decrease in work hardening due to slowing down of strain-induced martensite formation at high biaxial strains [Murr et al.(1982)]. This is because in biaxial tension, martensite formation is twice as fast as under uniaxial tension (Fig.2). Then, beyond a certain biaxial strain ratio, martensite formation reaches saturation. In fact, Hecker et al view deformation at or near balanced biaxial tension as being similar to lower temperature uniaxial deformation. The initially rapid martensitic transformation is not sustained to large strains, and premature local plastic instability results [Hecker et al.(1982)].

Strain distributions along 200mm length of are presented for the 0.50mm thick and 1.25mm thick sheets. Even with optimised tool geometry, strain gradients are present due to the presence of stress gradients caused by friction at the sheet/punch interface [Narutani(1989)]. The average distance between the major strain peaks is nearly constant and the values for 0.50mm thick and 1.25mm thick sheets respectively are 104±8mm and 105±9mm. The profiles display some asymmetry in the height of the major strain peaks. This is because when a strain peak develops into a localised neck (due to chance variations in local sheet thickness and/or metallurgical inhomogeneity), the other peak ceases to grow further causing the observed asymmetry. In view of the major and the minor strain gradients present, a constraint factor (f) is determined [Date et al.(1992)], viz.,

$$f = \frac{\varepsilon_{2peak} - \varepsilon_{2pole}}{\varepsilon_{1peak} - \varepsilon_{1pole}} \qquad (5)$$

Where ε_{2pole} and ε_{1pole} are the values of the true minor and major strains at the pole respectively, and ε_{2peak} and ε_{1peak} are the corresponding values at the strain peaks.

International Journal of Engineering Applied Sciences and Technology, 2018
Vol. 3, Issue 9, ISSN No. 2455-2143, Pages 37-42
Published Online January 2019 in IJEAST (http://www.ijeast.com)

$$\frac{df}{f} = \frac{d\varepsilon_{2peak} - d\varepsilon_{2pole}}{\varepsilon_{2peak} - \varepsilon_{2pole}} - \frac{d\varepsilon_{1peak} - d\varepsilon_{1pole}}{\varepsilon_{1peak} - \varepsilon_{1pole}} \quad (6)$$

Where dε's are variation in ε's. Fig.4 shows plots of f against ε_{2peak} for the six stainless steel sheets. The plot of the constraint factor was steep in the case of the 0.50mm thick sheet compared with the 1.25mm thick sheet due to the larger strain gradients present in the former steel. This is due to the lower strain hardening capability. Though plots are not shown, the plots of e_2/e_1 ratio at a particular distance against blank widths have also been plotted and analysed.

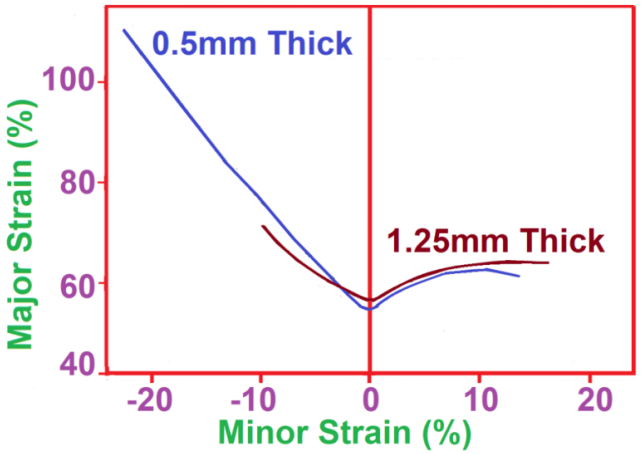

Fig.3. Plot comparing forming limit diagrams of 0.5mm thick and 1.25mm thick sheets

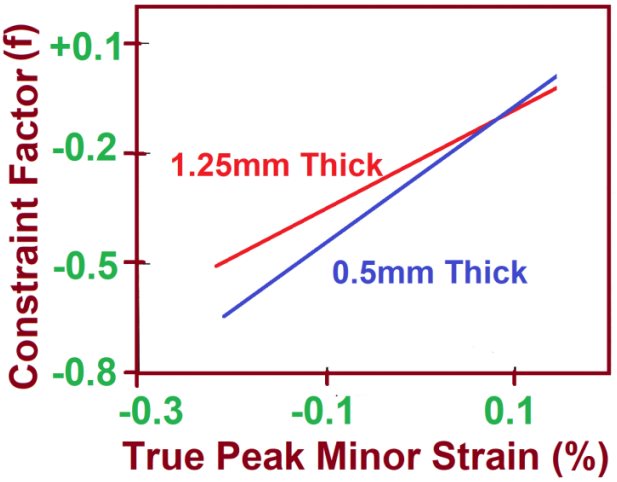

Fig.4 Comparison of the constraint factors of the 0.5mm thick and the 1.25mm thick sheets.

IV. Conclusion

From the present research, the following conclusions could be drawn.

(1) Both the sheets showed a similar type of tensile behavior. At any particular strain, amount of martensite formed was more in the 1.25mm thick sheet. Ductility of the 1.25mm thick sheet was greater than that of the 0.5mm thick sheet.

(2) All tensile property parameters decreased, displaying a drastic decrease above 673K mainly on account of a decrease in work hardening. It displayed very good ductility at 373K due to the absence of both martensite formation and DSA.

(3) It was inferred from average plastic strain rations that 0.5mm thick sheet expected to show somewhat greater deep drawability.

(4) Formability of 0.5mm thick sheet was lower in the stretch forming and plane strain forming conditions, but was superior in deep drawing region, when compared to that of 1.25mm thick sheet. The differences, however, did not exceed 5%.

(5) Formability of both the sheets decreased at high biaxial strains due to the saturation and slowing down of the martensite formation.

(6) The plot of the constraint factor was steep in the case of the 0.50mm thick sheet compared with the 1.25mm thick sheet due to the larger strain gradients present in the former steel.

V. References

[1] Hecker, S.S.; Stout, M.G.; Staudhammer, K.P.; and Smith, J.L. (1982). Effects of strain state and strain rate on deformation-induced transformation in 304 stainless steel: Part I Magnetic measurements and mechanical behavior. *Metallurgical Transactions*, 13A, (pp.619-626)

[2] Murr, L. E.; Staudhammer, K.P.; and Hecker, S.S.(1982). Effects of strain state and strain rate on deformation-induced transformation in 304 stainless steel: Part II - Microstructural study. *Metallurgical Transactions*, 13A, (pp.627-635)

[3] Narutani, T.(1989). Effect of deformation-induced martensitic transformation on the plastic behaviour of metastable austenitic stainless steel. *Materials Transactions (JIM)*, 30, (pp.33-45)

[4] Date, P.P.; and Padmanabhan, K.A.(1992). On the formability of 3.15mm thick low-carbon steel sheets. *Journal of Materials Processing Technology*, 35, (pp.165-181)

[5] Cios, G.; Tokarski, T.; Zywczak, A.; Dziurka, R.; Stepien, M.; Gondek, L.; Marciszko, M., Pawlowski, B.; Wieczerzak, K.; and Bala, P. (2017). The Investigation of Strain-Induced Martensite Reverse

Transformation in AISI 304 Austenitic Stainless Steel. *Metallurgical and Materials Transactions*, 48, (pp.4000-5008)

[6] Du Toit, M.; and Steyn, H.G. (2012). Comparing the formability of AISI 304 and AISI 202 stainless steel. *Journal of Materials Engineering and Performance*, 21, (pp.1491-1495)

[7] Satao, H.; Manabea, K.; Kondoa, D.; Weib, D.; and Jiang, Z. (2014). Formability of Micro Sheet Hydroforming of Ultra-fine Grained Stainless Steel. *Procedia Engineering*, 81, (pp. 1463-1468)

[8] Jayahari, L.; Sasidhar, P.V.; Reddy, R.; Balunaik, B.; Gupta, A.K.; and S. K. Singh (2014). Formability studies of ASS 304 and evaluation of friction for Al in deep drawing setup at elevated temperatures using LS-DYNA. *Journal of King Saud University-Engineering Sciences*, 26, (pp.21-31)

[9] Sivam, S.P.S.S.; Gopal, M.; Venkatasamy, S.; and Singh, S. (2015). Application of Forming Limit Diagram and Yield Surface Diagram to Study Anisotropic Mechanical Properties of Annealed and Unannealed SPRC 440E Steels. *Journal of Chemical and Pharmaceutical Sciences*, 9, (pp.15-22)

[10] Dehghani, F.; and Salimi, M.(2016). Analytical and experimental analysis of the formability of copper-stainless-steel 304L clad metal sheets in deep drawing," *International Journal of Advanced Manufacturing Technology*, 82, (pp.163-177)

[11] Reddy, A.C. (2017). Experimental and Numerical Studies on Formability of Stainless Steel 304 in Incremental Sheet Metal Forming of Elliptical Cups. *International Journal of Scientific and Engineering Research*, 8, (pp. 971-976)

[12] Andrade, M..; Gomes, O.A.; Vilela, J.M.C.; Serrano, A.T.L.; and de Moraes, J.M.D. (2004). Formability evaluation of two austenitic stainless steels. *Journal of Brazilian Society for Mechanical Sciences and Engineering*, 26, (pp.47-50)

[13] Sahu, J.; Chakrabarty, S.; Raghavan, R.; and Mishra, S.(2018). Investigations of size effect on formability and microstructure evolution in SS304 thin foils. *Journal of Strain Analysis in Engineering Design*, 53, (pp. 517-528 (2018)

[14] Kanniraj, A.(2008). Room temperature formability of AISI 304 stainless steel sheets. *Manufacturing Technology Today*, 7, (pp.15-20)